J Nanostruct 16(4): 4433-4451, Autumn 2026

RESEARCH PAPER

Synthesis, Spectroscopic Characterization, Antioxidant Activity and Molecular Docking Study of a Novel Schiff Base Silver (I) Micro/Nano-Complex Against A549 Lung Cancer Cells

Ghusoon Faidhi Hameed *, Duha M. Eidan, Zahraa Falah Khudair

Department of Chemistry, College of Education, University of Al-Qadisiyah, Diwaniyah, Iraq

ARTICLE INFO

Article History:
Received 06 May 2026
Accepted 05 July 2026
Published 01 October 2026

Keywords:
BCL-2 protein
Coordination chemistry
Molecular docking
Nanocomplex
Schiff base ligand

ABSTRACT

Due to their versatile structural characteristics and biomedicinal activities, Schiff base ligands have been extensively investigated, including in combination with metal complexes. We report here the synthesis of a novel Schiff base ligand (SBOSA) and its corresponding silver(I) complex and their application as potential antioxidant/anticancer agents. The ligand was prepared by condensation with Ag(I) ions, thereby forming a stable complex. The synthesised compounds were characterised in detail using physical and spectroscopy techniques, such as Fourier-transform infrared (FT-IR), 1H-NMR, 13C–NMR, UV–Vis, X-ray diffraction analysis (XRD), FESEM & magnetic susceptibility evaluation Spectral analyses supported the coordination of azomethine nitrogen and oxygen donor atoms to an Ag(I) centre, resulting in a stable square-planar complex geometry. The XRD and FESEM analyses also showed that the synthesized materials are nanoscale crystalline. Antioxidant and cytotoxic studies were conducted to assess the biological actions of these compounds. The free ligand was found to exhibit significant in vitro antioxidant activity using the DPPH radical-scavenging assay. The cytotoxic effects on A549 human lung adenocarcinoma cells were studied in vitro using the MTT assay. Concentration-dependent anticancer activity was demonstrated for both the ligand and its Ag(I) complex, although the free ligand showed better cytotoxic potency as well as selectivity against cancer cell lines than the corresponding metal complex. In addition, the molecular docking results against BCL-2 (PDB ID: 2XA0) indicated that the more stable protein–ligand complex represents an excellent binding mode. Highest binding occurred with the free ligand through hydrogen- bond interactions and Ag(I)through surface-enhanced geometrical stabilization by π–π stacking interactions.

How to cite this article
Hameed G., Eidan D., Khudair Z. Synthesis, Spectroscopic Characterization, Antioxidant Activity and Molecular Docking Study of a Novel Schiff Base Silver (I) Micro/Nano-Complex Against A549 Lung Cancer Cells. J Nanostruct, 2026; 16(4):4433-4451. DOI: 10.22052/JNS.2026.04.004

* *Corresponding Author Email: ghusoon.alabdullah@qu.edu.iq*

INTRODUCTION

Heterocyclic compounds are a class of organic molecules that consist of cyclic structures (i.e. rings) in which at least one atom within the ring structure is replaced with heteroatoms such as nitrogen, oxygen or sulfur instead of solely carbon atoms [1]. These systems are abundant in nature and often serve as scaffolds for medicinal chemistry, where structural diversity and electronic properties can be tailored . Heterocycles are among the basic elements in medicinal and functional materials design, since the presence of even a single heteroatom within a ring system significantly affects reactivity, stability, and biological activity. IntroductionSchiff bases are one of the most versatile classes of heterocyclic derivatives, which can usually be synthesized by the condensation between a carbonyl compound and a primary amine to produce an azomethine (–C=N–) functional group. Schiff bases are of great interest in the literature, mainly due to their easy preparation and structural versatility as well as good coordination with transition metal ions. In this way, these ligands establish stable metal complexes with different geometries and improved properties owing to the presence of donor atoms such as nitrogen or oxygen. [2,4]. Notably, Schiff base–metal complexes have been studied intensively for their diverse biological activities, including antimicrobial, antioxidant, and anticancer properties. Metal ion coordination generally improves the activity of the parent ligand by controlling some important molecular characteristics such as lipophilicity, redox properties and also interaction with biological targets [5,9] The present study aims to synthesize and characterize a novel Schiff base ligand (SBOSA) and its corresponding silver(I) complex using various spectroscopic and physicochemical techniques. In addition, the study investigates

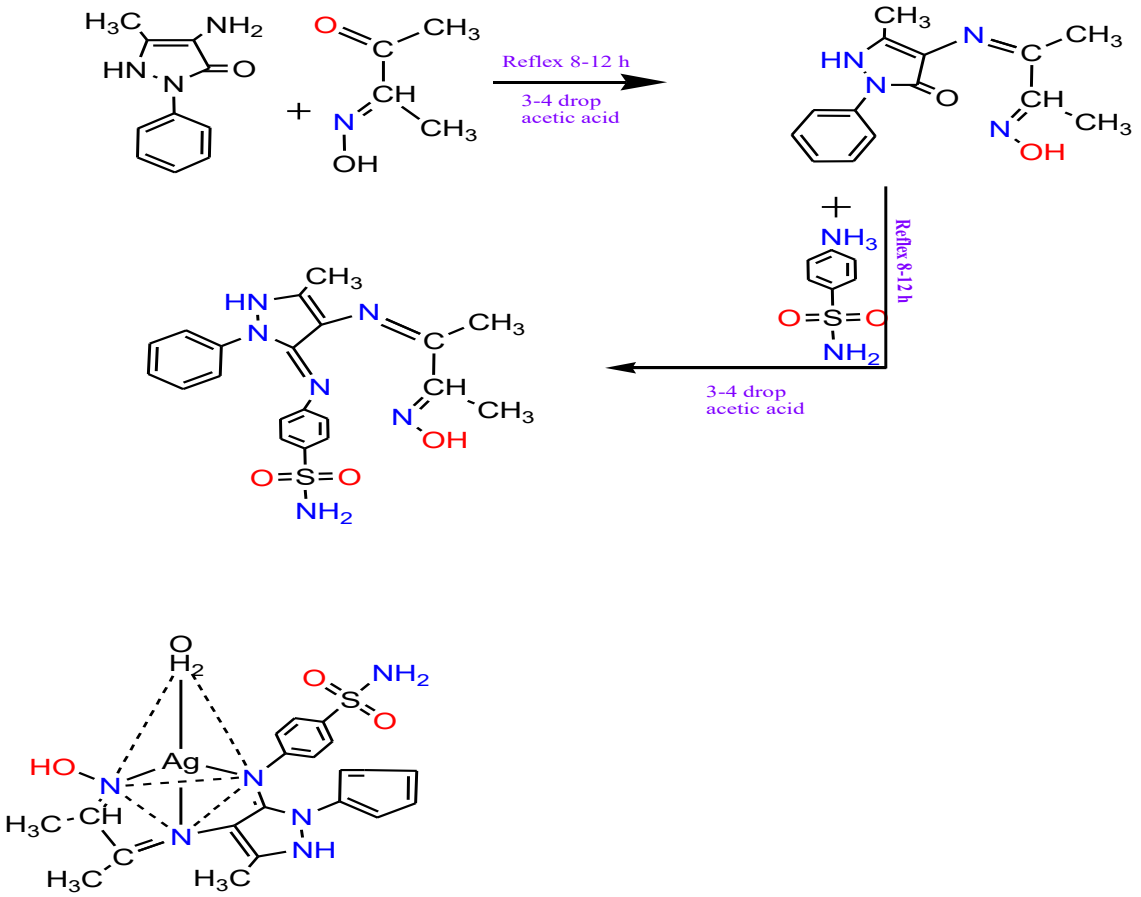

Fig. 1. Preparation of the Ligand.

the antioxidant and in vitro anticancer activities of the synthesized compounds against the A549 lung cancer cell line, alongside molecular docking analysis to evaluate their potential interactions with the BCL-2 protein as prospective bioactive therapeutic agents.

MATERIALS AND METHODS

Instruments, Materials, and Methods

We used only analytical grade substances. Compounds were characterized by FT-IR (Shimadzu, KBr, 4000–400 cm^{-1}), ^1H NMR (DRX 500 MHz, $DMSOd_6$), MS (Shimadzu Agilent 5975C), elemental analysis (EURO EA 3000), melting point (Electrothermal 9300), UVVis (200–1100 nm), SEM (MIRA3 TESCAN), XRD (D2 Phaser Bruker, 20–80° 2θ), and TGA (N_2 atmosphere). Antibacterial activity was assessed via agar well diffusion using a Memmert incubator.

Synthesis of the Schiff Base Ligand (SBOSA)

The Schiff base ligand (SBOSA) was synthesized through a condensation reaction between 4-aminoantipyrine and diacetylmonoxime using ethanol as the reaction medium and glacial acetic acid as a catalyst. Initially, 2.032 g (0.01 mol) of 4-aminoantipyrine was dissolved in 25 mL of absolute ethanol in a clean round-bottom flask under continuous magnetic stirring to obtain a clear homogeneous solution. In a separate beaker, 1.011 g (0.01 mol) of diacetylmonoxime was dissolved in 25 mL of ethanol. The diacetylmonoxime solution was then added gradually to the previously prepared 4-aminoantipyrine solution with constant stirring. Once the reactants were thoroughly mixed, 3–4 drops of glacial acetic acid were added as a catalyst to promote condensation and form Schiff bases. The resulting reaction mixture was heated

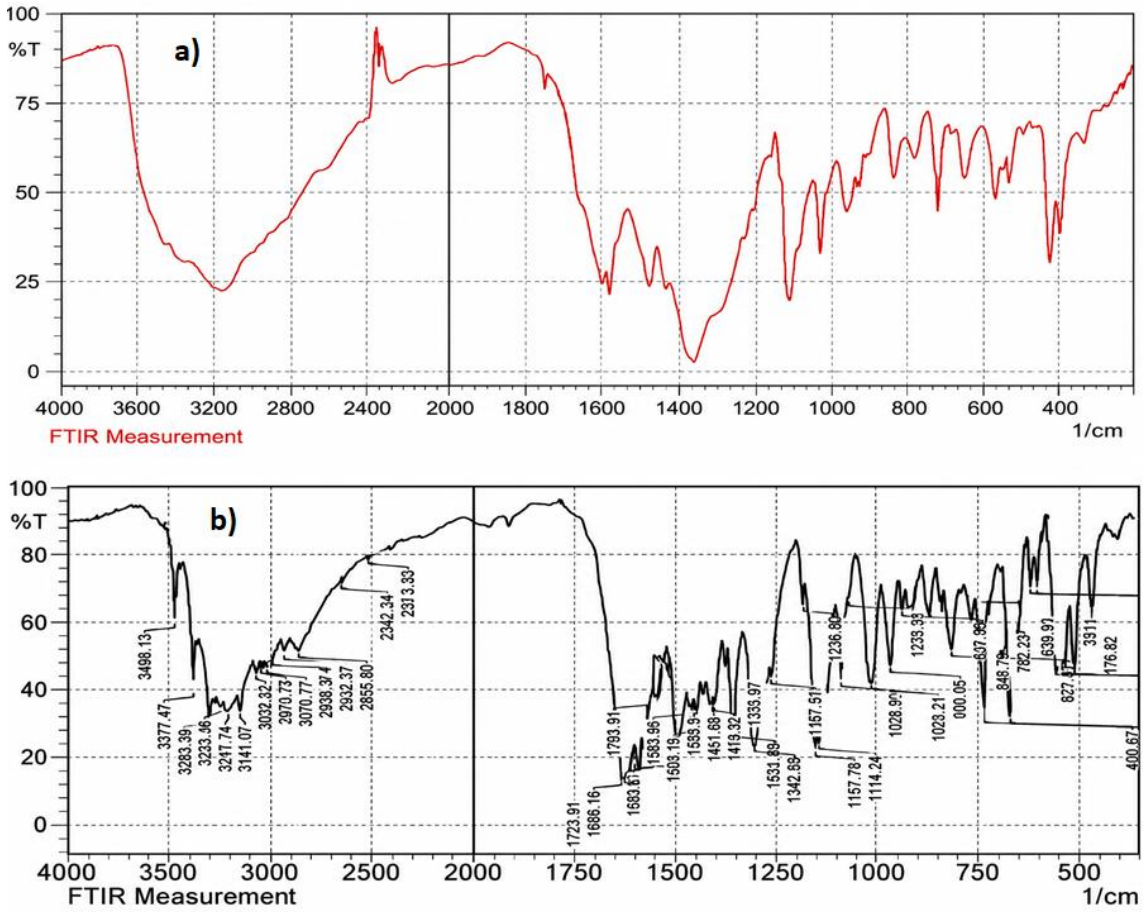

Fig. 2. The FTIR spectral data for the ligand SBOSA and Ag(I)-Complex.

under reflux for 8 h with continuous stirring to complete the reaction. After the reflux period, the reaction mixture was slowly cooled down to room temperature. Formation of a Schiff base ligand, confirmed by the formation of colored precipitate. It was filtered by vacuum filtration, washed multiple times with cold ethanol to remove excess starting materials and impurities, and then dried at room temperature. The crude product was then recrystallized from ethanol to yield the Schiff base ligand (SBOSA) in moderate purity. The last step was to collect the pure product, dry it completely at 70 °C, and weigh it. From there, we calculate the particulate yield in percentage [10].

Synthesis of SBOSA-Ag Complex

The Schiff base ligand (SBOSA) was synthesised using sulfanilamide in an ethanolic medium under reflux conditions, and the thiatosylate silver complex of the SBOSA ligand was named as [Ag(SBOSA)]…The first was that 2.86 g (0.01 mol) of the synthesised Schiff base ligand SBOSA(4-oxo-N-(3-O-benzyl)-sulfonic acid sodium salt;27,29a solution based on swift stirring for dissolving in which a homogeneous ethanol solution was prepared by means of ml measurement). Using a different approach, 1.722 g (0.01 mol) of sulfanilamide was solubilised in ethanol by dissolving it up to a volume of 25 mL . The sulfanilamide solution was then slowly dripped into the ligand solution while stirring continuously. A few drops of glacial acetic acid were added to the reaction mixture to introduce acidity, catalyse the reaction, and enhance complex formation. Refluxing the mixture (8 h) allowed full interaction of ligand with metal precursor to form our complex. Upon finishing the refluxing process, reaction mixture have cooled down to room temperature and desired SBOSA-Ag complex appears in a precipitate. The resulted solid product was isolated by filtration, washed with cold ethanol several times to remove any unreacted starting material or residues before drying at room temperature. The purified SBOSA-Ag complex was subsequently collected, quantified and dried to preserve in a desiccator for further physicochemical characterization as well as analytical studies [11].

MTT Assay on A549 Cell Line

In vitro antitumor activity against A549 human lung cancer cells of the synthesized compounds was tested using MTT assay. Cells cultured in standard conditions (37°C, 5% CO_2) with RPMI-1640 medium containing10% FBS and 1% penicillin/streptomycin. To do so, each of the compounds was dissolved in DMSO and prepared as stock solutions, from which a serial dilution with culture medium to reach the needed concentrations.A549 cells were seeded into 96-well plates at a density of 8×10^3 cells/well and incubated for 24 h to allow cell attachment[12]. After incubation, the medium was replaced with fresh medium containing different concentrations of the tested compounds, and the cells were incubated for an additional 24 h. Subsequently, the culture medium was removed, and 20 µL of MTT solution (1 mg/mL) was added to each well. Plates were incubated for 3–4 h at 37°C. The resulting formazan crystals were dissolved in 100 µL of DMSO, and absorbance was measured at 570 nm with an ELISA reader (Bio-Rad Laboratories). Cell viability was calculated using the Eq. 1:

$$\text{Cell Viability } (\%) = (A_{treated}/A_{control}) * 100 \quad (1)$$

RESULTS AND DISCUSSION

Synthesis of the Ligand (SBOSA)

The novel Schiff base ligand (SBOSA) was synthesized according to the general procedure detailed in the experimental section (2). Preparation of Ag(I)-Complex by Synthesis. Sliver (I) nitrate reacted with the ligand (SBOSA) in ethanol to form the Ag (I) Complex. The synthesis was conducted at a 1:1 (M: L) molar ratio of metal to ligand. Isolation, purification, and characterization

Table 1. lists the key FTIR bands of the ligand SBOSA and Ag(I)-Complex.

Compounds	υ(O-H)	υ(C-H) Aromatic	υ(C-H) Aliphatic	υ(C=N) Imine	υ(C=N) Thiazole	υ(M–N) υ(M–O)
Ligand (SBOSA)	3200.34 (s)	3132.18 (w)	2808.45 (w)	1630.09 (s)	1510.09 (s)	------
[Ag(SBOSA)] Cl	-------	3116.75 (w)	2923.88 (w)	1550.81 (s)	1596 (m)	547.75 (m) 455.17(m)

procedures were carried out on the isolated compound. The data regarding the elemental composition (CHN) and physical properties of the synthesized ligand (SBOSA), as well as Ag(I)-Complexit formed, are presented below in Table 1. The elemental analysis data confirm that the synthesized compounds are pure, as the results obtained match the expected molecular formulas of the compounds. Listing 1. Results of the elemental analysis and specifications of Ag(I)-Complex, combined with the ligand SBOSA.

Ag(I)-Complex with that of the free ligand (SBOSA). These changes provide strong evidence for metal-ligand coordination and are summarized as follows: The broad υ(O–H) band present in the ligand spectrum at 3425.34 cm^{-1} disappeared in the complex spectrum. This indicates the deprotonation of the phenolic hydroxyl group upon coordination to the palladium ion, acting as a monoanionic donor site[13]. A significant difference from that seen in the free ligand (1620 cm^{-1}) is a lowering (approximately 4-7 cm^{-1}) of the frequency for the major azomethine υ(C=N) band present in the complex. This lowering of frequency is indicative of coordination through the nitrogen atom of the imine group, and an associated decrease in the bond order of the nitrogen [14]. Two bands in the far-infrared region of the complex spectrum were also observed at 547.75 cm^{-1} and 455.17 cm^{-1} as shown in Fig. 2. These bands are assigned to the υ(M-N) and υ(M-O) stretching vibrations, which result from the interaction of the palladium ion with the deprotonated phenolic oxygen and azomethine

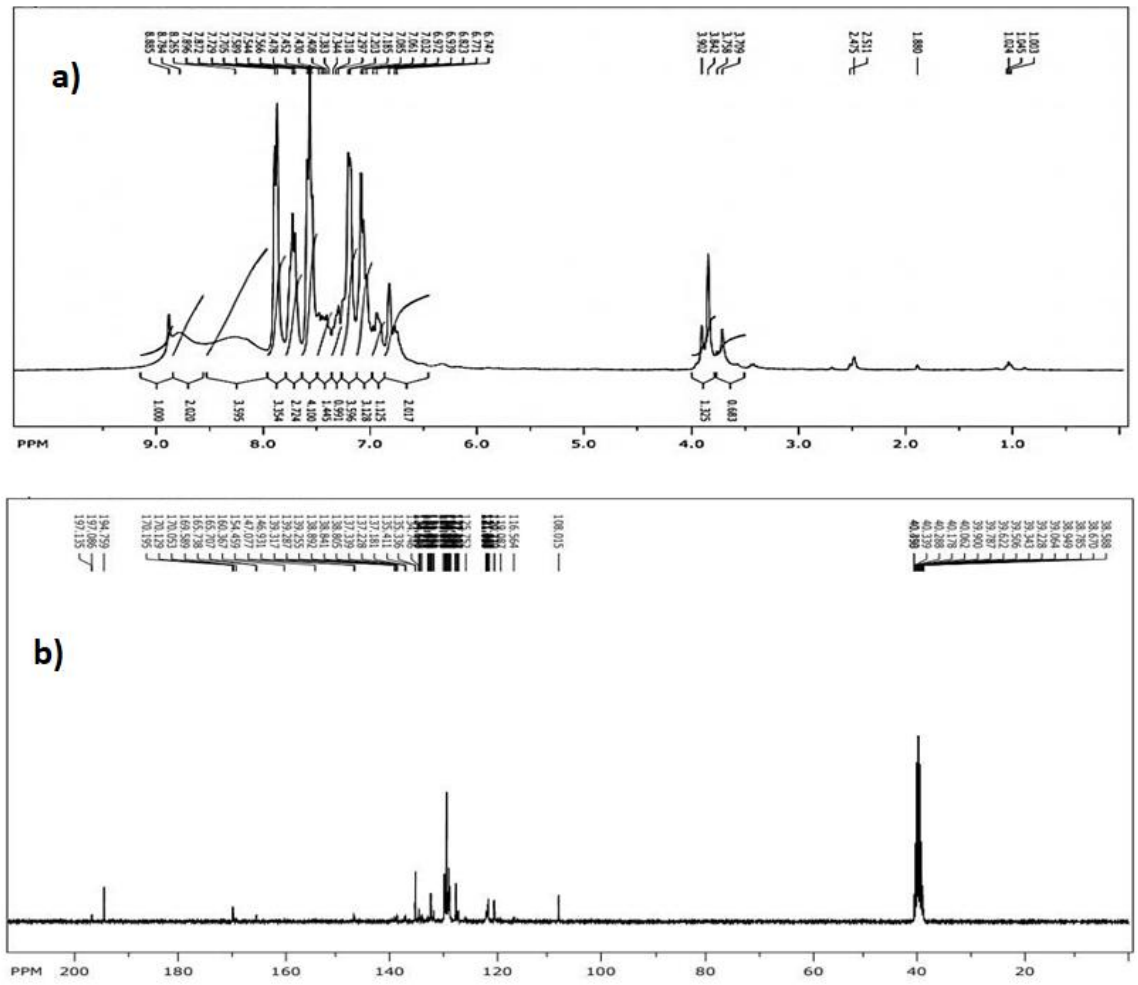

Fig. 3. a) ^{1}H-NMR & b) ^{13}C-NMR spectral data for the ligand SBOSA.

nitrogen atoms of the ligand, respectively [15].

Nuclear Magnetic Resonance (^{1}H -NMR) Spectroscopy

^{1}H-NMR Spectrum of the Ligand (SBOSA)

The ^{1}H-NMR spectrum of the prepared Schiff base ligand (SBOSA), shown in Fig. 3, provided clear evidence for the proposed molecular structure through the appearance of the expected proton signals. A singlet signal observed at δ 3.902 ppm integrating for two protons was assigned to the methylene (-CH_2-) group originating from the methylenedianiline fragment. The phenolic hydroxyl proton appeared as a singlet at δ 6.747 ppm corresponding to one proton. The aromatic protons of the phenolic ring were detected as a multiplet in the range δ 7.032–7.085 ppm, integrating to 4 protons. Formation of the Schiff base linkage was confirmed by the appearance of a characteristic singlet at δ 8.784 ppm assigned to the azomethine proton (-CH=N-). In addition, the aromatic protons of the methylenedianiline phenyl rings appeared as multiplet signals in the region δ 7.185–7.318 ppm corresponding to

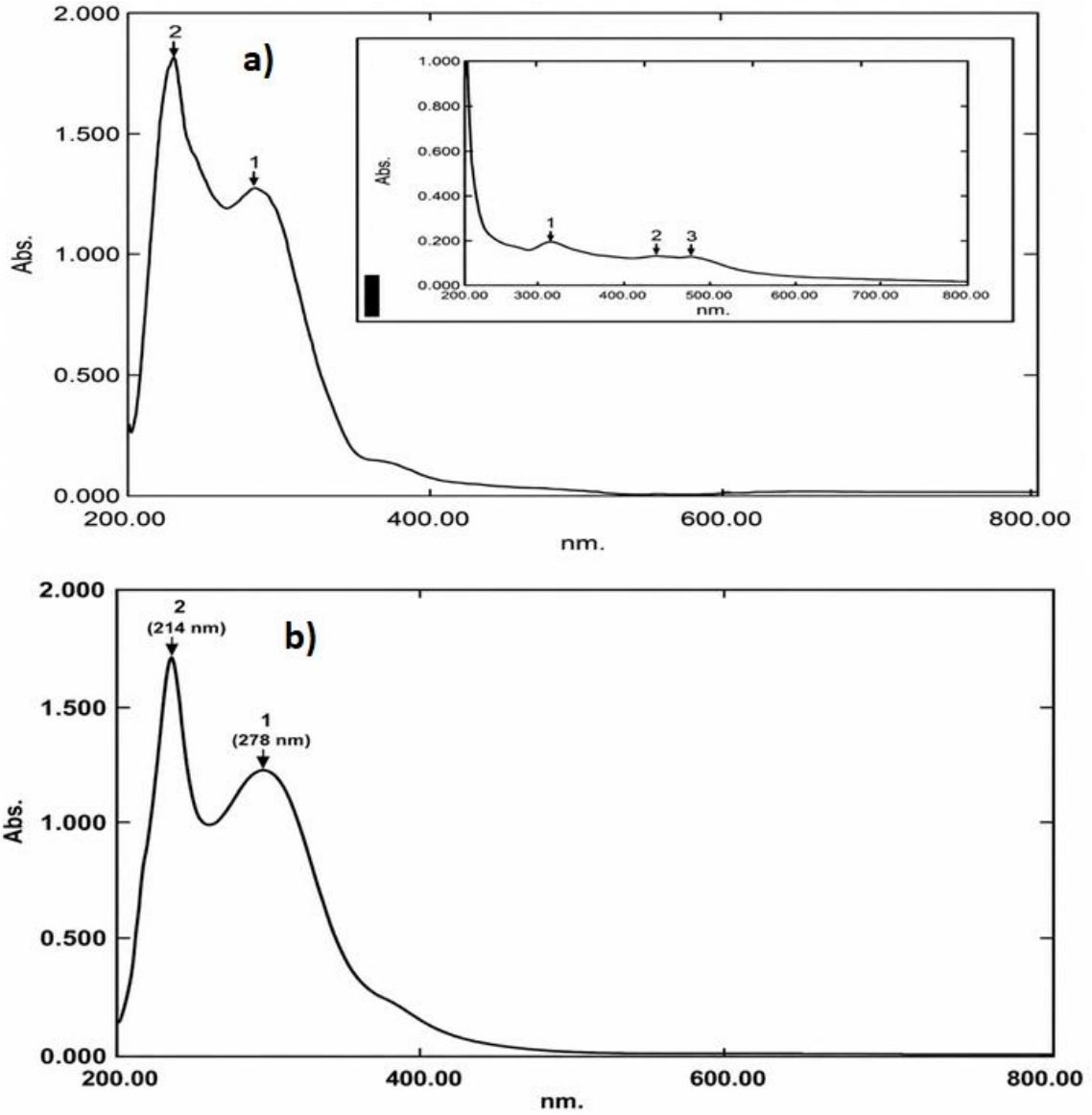

Fig. 4. The Uv-Vis. spectrum data for the a) ligand SBOSA and b) Ag(I)-Complex.

eight protons. Furthermore, the aromatic protons associated with the benzylidene moiety were observed as multiplets at δ 7.344–7.589 ppm, with an integration of 10 protons.

^{13}C-NMR Spectrum of the Ligand (SBOSA)

The ^{13}C-NMR spectrum of the synthesized ligand (SBOSA) further supported the proposed chemical structure through the appearance of characteristic carbon resonances. The methylene carbon atom (C14) derived from the methylenedianiline fragment appeared at δ 40.398 ppm. The azomethine carbon atoms (C7, C21, and C28) were observed at δ 154.459, 160.367, and 165.707 ppm, respectively, confirming the formation of the Schiff base functionalities.Signals corresponding to the phenolic ring carbons (C1–C5) were detected at δ 108.015, 116.564, 119.087, and 125.752 ppm. The aromatic carbons belonging to the two phenyl rings of the methylenedianiline moiety (C8–C13 and C15–C20) appeared within the region δ 134.746–135.336 ppm. In addition, carbon atom C6 exhibited a resonance signal at δ 197.135 ppm. The aromatic carbons of the benzylidene rings were identified in the range δ 135.411–138.841 ppm. Furthermore, two characteristic signals observed at δ 146.931 ppm and 194.759 ppm were assigned to the carbon atoms of the thiazole ring (C35 and C37), respectively, providing additional confirmation for the ligand structure.

Spectroscopic Characterization of the Ligand (SBOSA)

The electronic spectrum of the free ligand

Table 2. Peaks Absorption Values, Magnetic Momentum and Expected geometry for ligand SBOSA and Ag(I)-Complex.

Compounds	λ (nm)	υ^{-} (cm^{-1})	Transitions	μeff (B.M)	Geometry
Ligand (SBOSA)	226	44247	π-π*	-	-
	291	34364	n-π*		
[Ag(SBOSA)]Cl	247	40485	Intra Ligand	0.00 (dia)	Square planar dsp^2
	313	31948	Intra Ligand		
	537	18621	$A_1g \rightarrow {}^1Eg^1$		
	604	16556	$A_1g \rightarrow {}^1B_1g^1$		
	664	15060	$A_1g \rightarrow {}^1A_2g^1$		

Table 3. Presents the diffraction angles θ, d-spacing values, and relative intensities for each Ligand (SBOSA) Ag(I)-Complex nanocomposite and its complex.

	No.	Pos. °2Θ.(Radian)	d-spacin A°	Intensity In	[%] Rel. Int
(SBOSA)	1-	10.904	8.11608	1706.28	41.62
	2-	11.2209	7.88567	1305.30	31.84
	3-	17.5677	5.04846	3102.09	75.66
	4-	18.2014	4.8740	989.96	24.15
	5-	20.8996	4.25055	2394.09	58.40
[Ag(SBOSA)H_2O]	1-	29.1273	3.06596	165.50	13.66
	2-	38.2806	2.35126	1211.87	100
	3-	44.4698	2.03735	518.27	42
	4-	64.5588	1.44357	239.94	19.72
	5-	77.4972	1.23070	230.94	19.06

SBOSA, recorded in ethanol at concentrations of 10^{-3} and 10^{-4} M, exhibits two well-defined absorption bands Fig 4, confirming the presence of its characteristic chromophores. The first high-intensity band observed at 226 nm (λmax, ε = L mol^{-1} cm^{-1}) is assigned to a π→π* transition in the conjugated aromatic ring system of the ligand. Electronic absorption spectroscopy in the UV-Vis region (200-900 nm) was employed to characterise the electronic structure of the free ligand L5H and its corresponding Ag(II) Complex, providing critical insights into coordination-induced changes and the geometry of the metal centre. This is a typical feature of organic aryl compounds. The second, lower-energy band at 291 nm (λmax) can be clearly ascribed to a transition from the nitrogen lone-pair (n) to the anti-bonding π* orbital of the azomethine (-CH=N-) group; therefore, it represents a direct spectroscopic indicator of the azomethine (imine) functional group that is expected to serve as the primary donor site for metal binding. The clear observation of this transition provides evidence for the availability of non-bonded electrons for donation to the metal centre, demonstrating the ligand's potential to act as a chelate. Spectroscopic Characterization and Structural Determination of the Palladium Complex [(SBOSA) Ag]. The modification of the complex's spectra relative to the free ligand demonstrates that coordination has occurred and indicates the structure of the complex. Complex Absorption Spectra Show Expected Ligand-Centred Absorptions at Lower Energy than Expected: The free ligand shows absorptions in the UV-Vis spectrum that would be centred on the ligand. These absorptions are shifted to lower energies with the palladium complex, with absorptions at 247 nm (40,485 cm^{-1}) and 313 nm (31,948 cm^{-1}). This red-shifted, or bathochromically shifted, absorption indicates coordination between a metal atom and a ligand molecule. The shift in the n→π* band for the azomethine is a further indication that the imine nitrogen has formed a bond with Ag(I), as coordination lowers the energy of both the nitrogen lone pair and the π* system. Bands corresponding to d-d Transitions and Square Planar Geometry: The most conclusive evidence for this is the presence of three different, low-energy absorptions in the visible region of the spectrum, occurring at 537 nm (18,621 cm^{-1}), 604 nm (16,556 cm^{-1}), and 664 nm (15,060 cm^{-1}). These bands do not appear in the ligand spectra and are therefore assigned to spin-allowed d-d (or ligand field) transitions within the d8 electronic

Table 4. presents the diffraction angles, full width at half maximum (FWHM) values, and crystallite sizes of the ligand (SBOSA) and its metal complex.

Compound	No.	Peak Position °2Θ	Peak Width (FWHM)	D Crystallite size(nm)	Rel. Int. [%]	Lattice Strain
(SBOSA)	1-	10.904	0.10476	56.44659	41.62	0.00675
	2-	11.2209	0.0984	84.69279	31.84	0.00437
	3-	17.5677	0.1968	42.64392	75.66	0.00556
	4-	18.2014	0.2464	34.08943	24.15	0.00671
	5-	20.8996	0.1476	57.13962	58.40	0.00349
[Ag(SBOSA)H_2O	1-	29.1273	0.1476	58.05812	13.66	0.00248
	2-	38.2806	0.2952	29.74101	100	0.00371
	3-	44.4698	0.2952	30.35452	42	0.00315
		64.5588	0.1968	49.85417	19.72	0.00137
		77.4972	0.3000	35.45595	19.06	0.00163

configuration of Ag (I). The only geometry that produces all three possible electronic transitions ($^1A_1g \rightarrow {}^1Eg$, $^1A_1g \rightarrow {}^1B_1g$, $^1A_1g \rightarrow {}^1A_2g$) is the square planar geometry, a result of the very strong coordination influence that creates a large splitting of the d-orbital energies in d^8 metal complexes like those of Ag (I). The triplet transition pattern is a clear indication that the complex has a square planar configuration and can be used to eliminate any consideration of the tetrahedral or octahedral configurations as possibilities for this compound, since both of the latter will have different numbers and patterns of d-d transitions. The electronic spectral information presented tells a clear story about the chromophore groups present within the ligand. The azomethine group is the primary donor site for the ligand. Ag coordination gives rise to observable contrast in the ligand-centred bands and therefore is a clear sign of successful delivery. Thirdly, the intrinsic spectral characteristics of these triplet d–d band transitions constitute strong evidence that they officially serve as spectroscopic proof by being square planar-form complexes in solution with Ag(I)-Complex. In turn, realization of this structural assignment may help in understanding the puzzling diamagnetic nature and unique chemical reactivity which suggests further synthetic possible applications as shown in

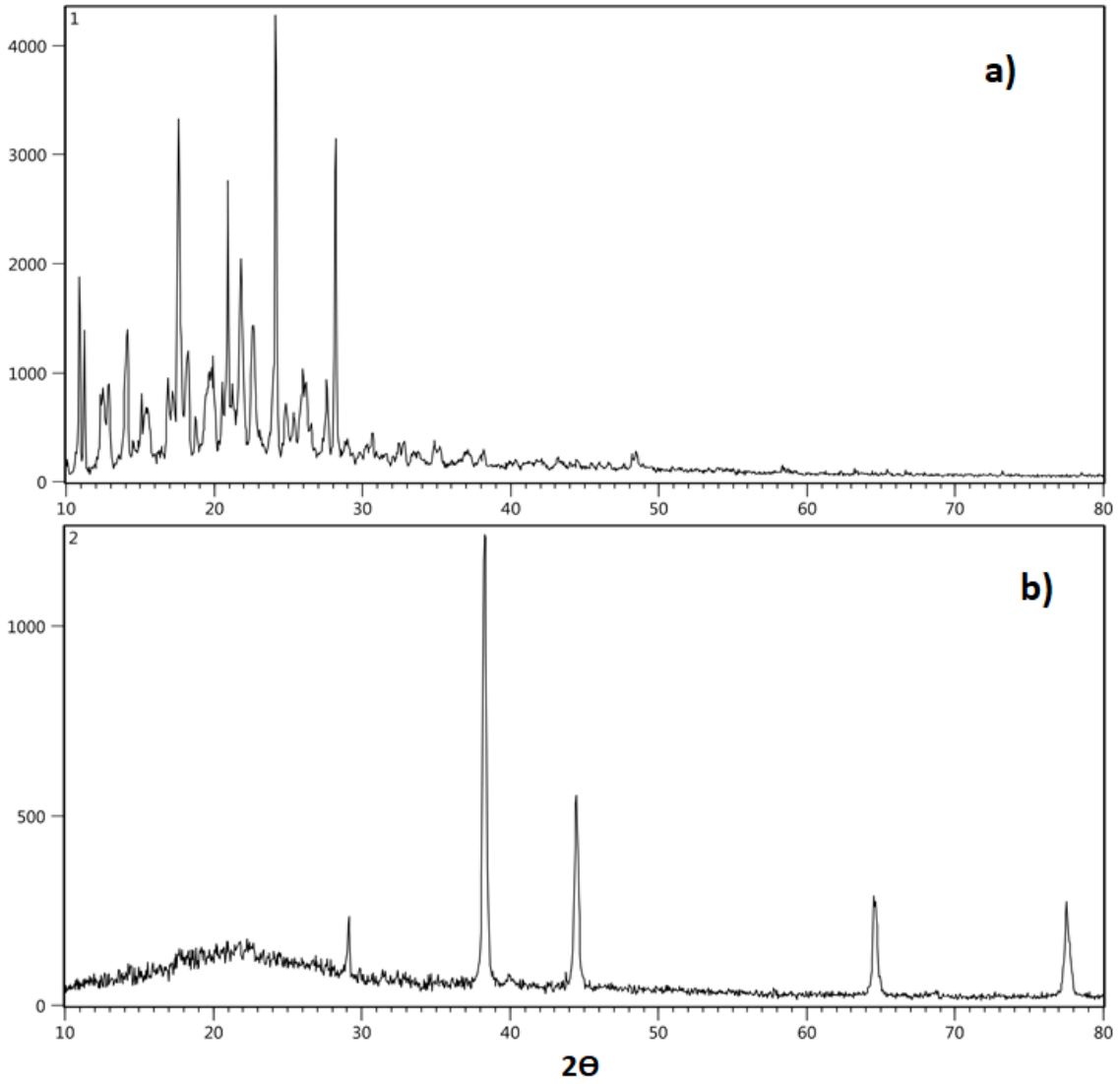

Fig. 5. X-Ray for the a) ligand SBOSA and b) Ag(I)-Complex.

Table 2 [16, 17].

X-ray Diffraction Analysis (XRD)

The ligand (LA) and its complex in the solid state were studied by X-ray diffraction analysis within an angular range of 2 θ = 10°–80°. Through these diffraction measurements, we obtained critical information such as crystalline structure and crystallite size, in addition to the overall purity of our synthesized compound. Due to a number of factors such as micro-strains arising from lattice deformation, crystal faulting due to structural distortions and domain size or domain size distribution, the diffraction peaks of the prepared compounds appeared broadened. In XRD analysis, the needle exhibits sharp, intense diffraction peaks, suggesting an ordered crystalline lattice, as supported by its crystalline or semi-crystalline nature. On the contrary, its wide and weak peaks revealed an amorphous character of this compound. The formula for calculating the crystallite size and interplanar space (d-spacing)

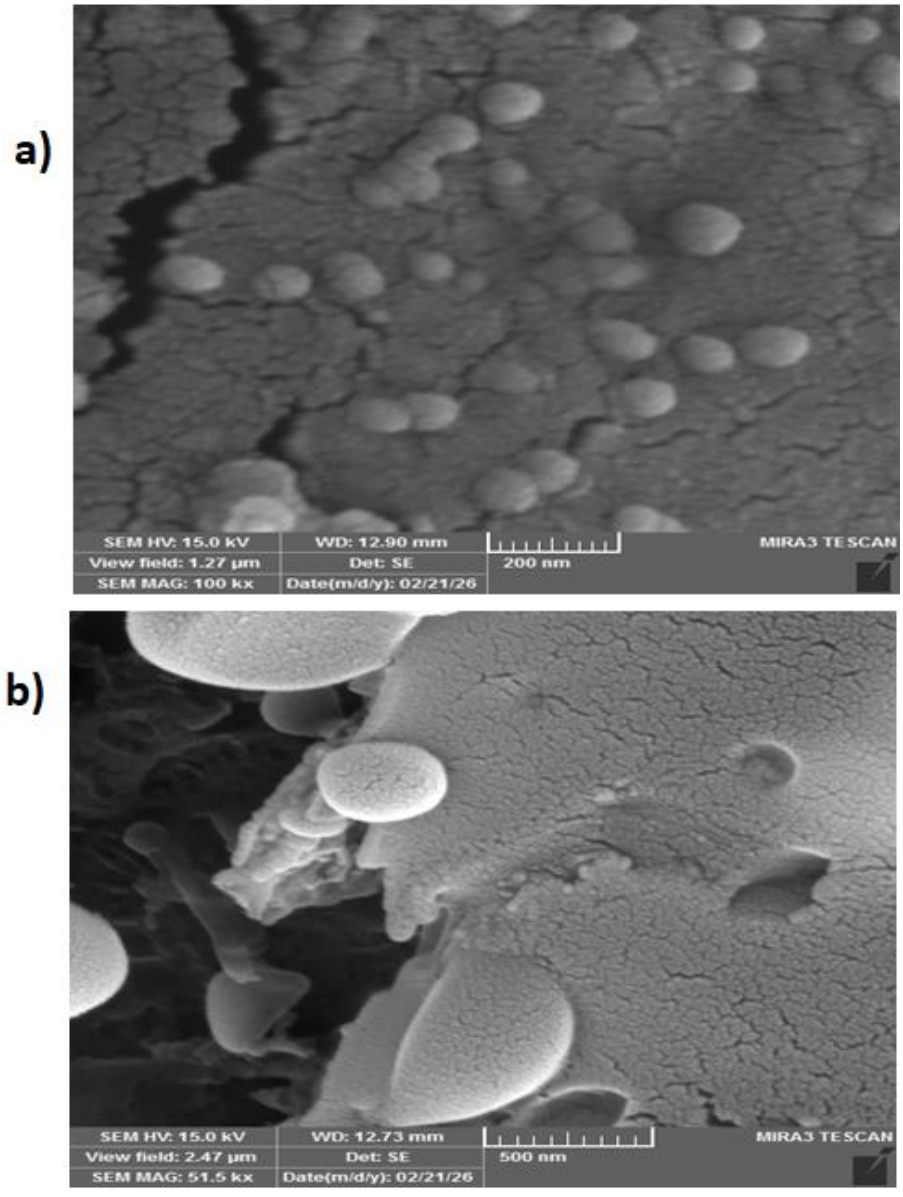

Fig. 6. Scanning electron microscope images of a) (SBOSA) and b) Ag(I)-Complex.

was as Eq. 2:

$$d = n\lambda/(2 \sin \theta) \quad (2)$$

where (d) represents the distance between crystal planes, (n) is the diffraction order, (λ) is the wavelength of the incident X-ray radiation ((1.540598 Å), and (ɵ) is the diffraction angle. Bragg's law was also employed to determine the interplanar spacing (d-spacing), where an inverse relationship was observed between the d-spacing values and the diffraction angle. The highest d-spacing value corresponded to the diffraction peak with the maximum intensity (100%) and the lowest diffraction angle. Comparison between the ligand diffraction peaks and diffraction angles showed that at the highest intensity peak, the d-spacing value was 2.35 Å, while the corresponding diffraction angle was the lowest among the recorded angles, with a value of 38.28°, as presented in Table 3.

The crystallite size of the ligand (SBOSA) and its metal complexes was calculated using the Debye–Scherrer equation, as shown Eq. 3:

$$D = K\lambda/(\beta \cos\theta) \quad (3)$$

where (D) represents the average crystallite size, (K) is the shape factor (Scherrer constant) with an approximate value of 0.9, λ is the wavelength of the incident X-ray radiation ((Cu K_α= 0.15056 nm, β is the full width at half maximum (FWHM) of the diffraction peak, and (ɵ) is Bragg's diffraction angle as shown in Table 4.

Analysis of the X-ray diffraction (XRD) measurements given in the Fig. 5 demonstrated that, upon coordination with a ligand bound to each metal ion, the relative crystalline structure showed different affinity for complexation. XRD Confirmation of Materials Crystallinity. The diffraction pattern captured in PR-PES (Fig. 5) of the LA shows a distinct substructure with clear pulse surface facets. A similar pattern was observed for the Ag(I) complex as well, in which nearly perfectly sharp peaks and a few broad ones appeared, along with a predominated intensity ratio dependence emerging from this characteristic crystal trend. It showed that the positions & intensities of diffraction peaks from experimental investigations matched one-to-one with standard international diffraction data cards, indicating ratios observed corresponding to the main related synthesised compounds. Furthermore, no additional peaks were detectable in relation with foreign impurities or detrimental phases. XRD data analysis indicated that all synthesized compounds were of nanoscale because the calculated crystallite sizes are below 100 nm.

Scanning Electron Microscopy (SEM) Analysis

Field Emission Scanning Electron Microscopy (FESEM) was employed to obtain detailed information about the surface morphology, particle size, particle shape, crystalline structure, and particle aggregation behavior of both the ligand and its metal complex. FESEM is considered one of the most important characterization techniques for investigating surface properties, as the physical characteristics and activity of the ligand and complex depend mainly on the nature and morphology of their surfaces.The FESEM measurements were carried out using a cross-sectional scale of 500 nm and a magnification power of Mag = 70.00 KX. FESEM images of the ligand were clustered in granular shapes, with an average particle size between 90.71 and 99.40 nm (95.06 ±). The agglomeration of particles was due to a clustering process, in which the primary nanoparticles aggregate along with each other which is unavoidable because high temperatures are used during synthesis. In contrast, FESEM image of silver complex Ag(I): by analysis with the argentisome reveals that; Most of these nanoparticles are spherical in shape and size below 100 nm which confirms i.e., they were nanoscale particles. The effective surface area increases

Table 5. Elemental analysis of the ligand (SBOSA) and complex Ag(I).

compound	M. Wt g/mol	Calc. (Found)%				
		C	H	N	S	M
Ligand (L)	440	57.27	5.45	19.6	7.27	-
$S_3O_6N_{24}H_{21}C$		56.41	5.02	19.65	2.71	
[Ag(L) H_2O]	548	45.98	4.37	15.32	5.83	19.70
$O_3SAg_6N_{24}H_{21}C$		30.07	4.08	13.52	1.98	19.6

because of the nanoscale dimensions leading to an increase in quantum effects that create new energy levels and yield electron mobility. These unique properties provide considerable advantages for potential applications in various industrial fields, including thermal and electrical conductivity applications, as well as in medical and pharmaceutical fields such as anticancer and antibacterial applications. Therefore, further future studies are recommended to investigate these important properties and explore their possible industrial and biomedical applications as shown in Fig. 6. [18].

C.H.N.S Elemental Analysis

The percentages of carbon, hydrogen, nitrogen, and sulfur elements for the synthesized ligand and its metal complexes were determined using C.H.N.S elemental analysis in order to confirm the proposed chemical structures. The analysis was carried out using a Elementar Analysensysteme GmbH instrument. The obtained experimental results showed good agreement with the theoretically calculated values, confirming the correctness of the ligand structure, the validity of the molar ratios used in the preparation of the metal complexes, and the accuracy of the proposed structures of the synthesized compounds. The results of the C.H.N.S elemental analysis for the ligand and its metal complexes are presented in the Table 5.[19].

Radical 1,1-diphenyl-2-picrylhydrazil DPPH assay
A- Principle

The free radical scavenging activity of antioxidant substances is often measured using (1,1-diphenyl-2-picrylhydrazil radical DPPH), a stable free radical. The non-radical form of DPPH (DPPH-H) is formed when an antioxidant donates hydrogen to a solution of DPPH (DPPH-) in ethanol. The spectrophotometric measurement of this process reveals a transition from a purple to a yellow hue. At a wavelength of 517 nm, the purple color's fading is tracked as shown in Figs. 7-9. One may use DPPH to assess the scavenging activity against free radicals as shown in Tables 6-9 [20].

Calculation

Inhibition %= (Abs. of control – Abs. of sample/ Abs. of control) × 100

Where:

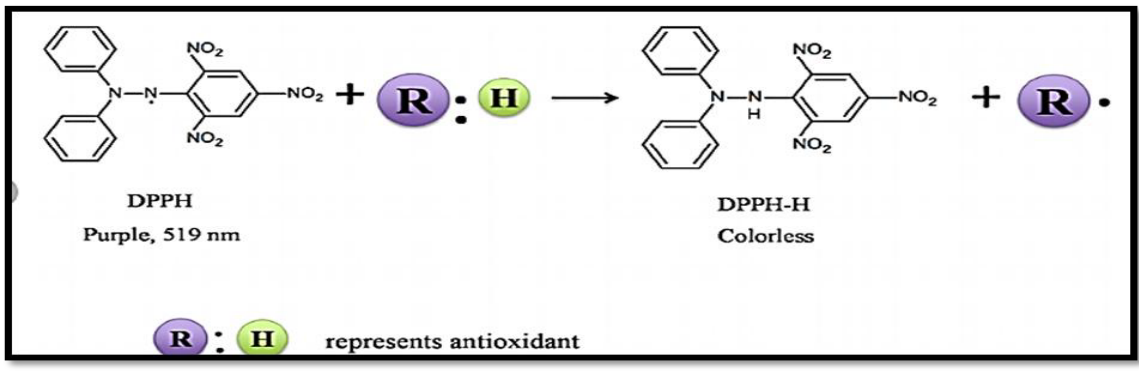

Fig. 7. Reaction mechanism of 2,2-diphenyl-1-picrylhydrazyl (DPPH) with antioxidant. R: H = antioxidant radical scavenger; R = antioxidant radical [21].

Table 6. Evalution of the antioxidant activity of the ligand (SBOSA) in vitro.

Con.	Absorbance	Inhibition percentage
Control	1.9	0 %
Ascorbic acid (vt.c)	0.13	93.15 %
100 mg/ml	0.43	77.36 %
50 mg/ml	0.44	76.84 %
25 mg/ml	0.85	55.26 %
12.5mg/ml	1.06	44.21 %
6.25 mg/ml	1.08	43.15 %

Abs control : Absorbance of the control solution(DPPH with ethanol)

Abs sample : Absorbance of the sample (extracts solution)

Measure Antioxidant Activity

Cytotoxic Activity Against A549 Lung Cancer Cells

The cytotoxic activities of SBOSA and its corresponding Ag(I)-Complex against the A549 human lung adenocarcinoma cell line were evaluated using the MTT assay after 24 h of incubation. Cell viability percentages were calculated relative to untreated control cells, which were considered as 100% viable.The obtained results demonstrated that the free ligand SBOSA exhibited a pronounced concentration-dependent cytotoxic effect against A549 cells. And by preventing cancer 1to 80 µg/mL penetration and at the same time in a percentage if we look to that on (78%–53%) decrease decreasing gradually. Also the reduction of cell viability fitted well with the strong antiproliferative activity by SBOSA against A549 lung cancer cells within this concentration range. The low standard deviation values from replicate measurements re-confirm the reproducibility and reliability of these experimental data. The incorporation of azomethine functional group and conjugated

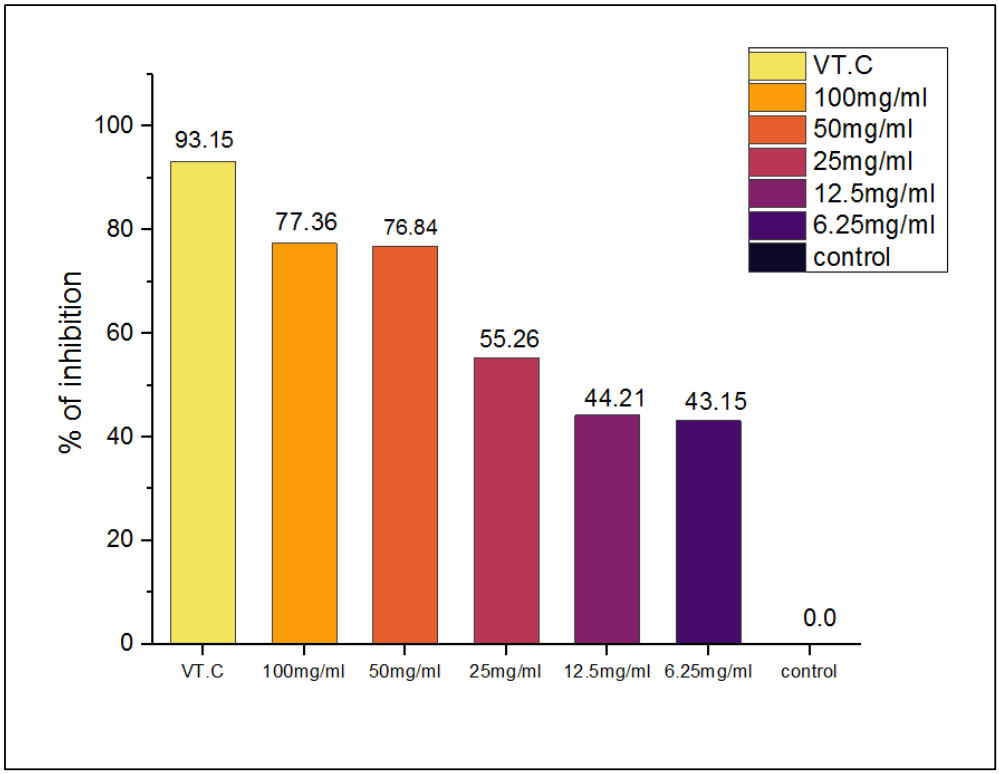

Fig. 8. Antioxidant activity for the ligand (SBOSA).

Table 7. Evalution of the antioxidant activity of the complex Ag (SBOSA) in vitro.

Con.	Absorbance	Inhibition percentage
Control	1.9	0 %
Ascorbic acid (vt.c)	0.13	93.15 %
100 mg/ml	0.65	65.78
50 mg/ml	0.66	65.26
25 mg/ml	0.71	62.63
12.5mg/ml	0.82	56.84
6.25 mg/ml	0.94	50.52

aromatic system in SBOSA may have reinforced its cytotoxic activity by facilitating interaction with important intracellular biomolecular target(s). Cytotoxicity of Schiff base compounds can occur via several mechanisms, such as action on DNA, generation of reactive oxygen species (ROS), inhibition of acetylcholinesterase and mitochondrial dysfunction [7]. The concentration-dependent decrease in viability indicates that the higher the concentrations of SBOSA, this contributes to more efficient cellular uptake and biological interaction which led to greater inhibition capability towards cell growth. On the other hand, Ag(I)-Complex showed lower cytotoxic activity against A549 cells. Cell viability at the concentrations used was relatively high with a decrease from 95% of total cellular function (0 µg/mL) to 74% at 40 µg/mL. While concentration-dependent inhibition was observed with the complex, it had significantly lower anticancer activity than SBOSA in free solution. These results indicate that at the experimental

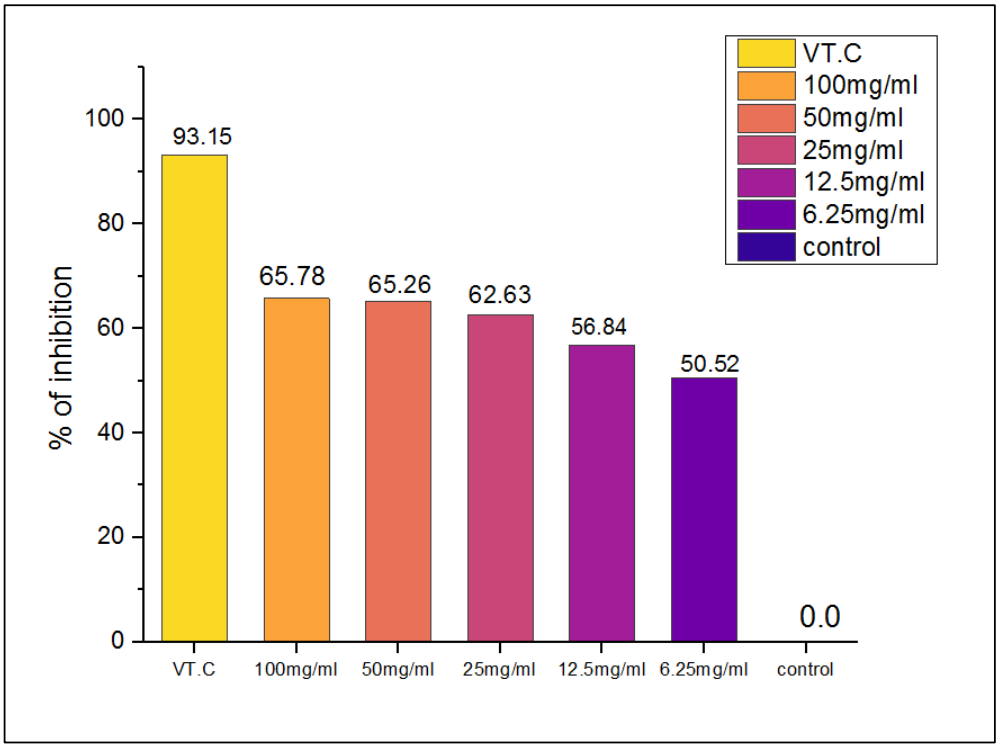

Fig. 9. Antioxidant activity for the complex Ag(SBOSA).

Table 8. Cytotoxic Activity of SBOSA Against A549 Lung Cancer Cells by MTT Assay.

	A549 SBOSA					
Concentration (µg/ml)	80	40	20	10	1	0
OD	0.217	0.304	0.325	0.339	0.312	0.439
	0.243	0.316	0.343	0.319	0.347	0.435
	0.249	0.337	0.324	0.367	0.341	0.477
	0.236	0.349	0.308	0.338	0.399	0.45
mean	0.236	0.327	0.325	0.341	0.350	0.450
SD	0.0120	0.0176	0.0124	0.0171	0.0314	0.0164
Cell viability %	53	73	72	76	78	100

conditions used, complexation with Ag(I) decrease total cytotoxic potency against A549 lung cancer cells. The change in biological activity between SBOSA and the Ag(I)-Complex is likely mediated by modifications of physicochemical properties that arise as a result of metal coordination. The extent of Ag(I) ions coordination can modulate lipophilicity, molecular geometry and redox properties along with membrane permeability that influence the interaction in intracellular biological targets directly. These findings further indicate that the unimolecular free ligand SBOSA is likely to be more vulnerable to structural flexibility and cellular interactiveness than its corresponding metal complex throughout this study. Moreover, steric hindrance from the coordination with metal center is likely to restrict accessibility of active biological donor sites that are involved in cytotoxic mechanisms.In conclusion, the overall SBOSA has significantly higher antiproliferative and cytotoxic effects on A549 lung cancer cells than Ag (I)-Complex as indicated by MTT assay results as shown in Fig. 10. Taken together, our results underscore the biological activity of SBOSA, making it an attractive candidate for future anticancer investigations. In addition, other studies should be performed related to the molecular basis of anticancer activity through apoptosis assays by measuring reactive oxygen species and Cell Cycle Analysis as well as performing a Molecular Docking [23,26]. Ag(I)-SBOSA exhibited weaker cytotoxic activity. Cell viability remained relatively

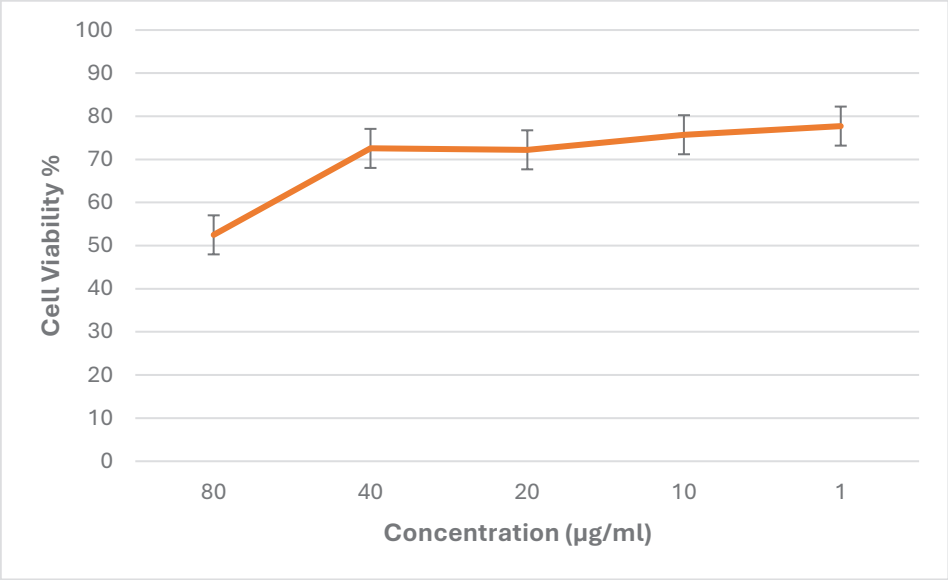

Fig. 10. Effect of SBOSA concentration on A549 Cell Viability by MTT Assay.

Table 9. Cytotoxic Activity of complex Ag(SBOSA) Against A549 Lung Cancer Cells by MTT Assay.

	A549					
Concentration (µg/ml)	40	20	10	5	1	0
OD	0.319	0.344	0.409	0.425	0.471	0.439
	0.341	0.348	0.416	0.414	0.402	0.435
	0.333	0.331	0.405	0.414	0.403	0.477
	0.338	0.354	0.37	0.418	0.425	0.45
mean	0.333	0.344	0.400	0.425	0.425	0.450
SD	0.0084	0.0084	0.0178	0.0139	0.0280	0.0164
Cell viability %	74	77	89	93	95	100

high across the tested concentrations, decreasing from 95% at 1 µg/ml to 74% at 40 µg/ml.

Molecular docking

Molecular docking analysis that was used in this study is an advanced computational tool to find binding interaction of synthesized compounds against active BCL-2 protein (PDB ID: 2XA0). The conformational properties of the proteins were verified with Ramachandran plot analysis before carrying out docking calculations. The results demonstrated that the structure is good because

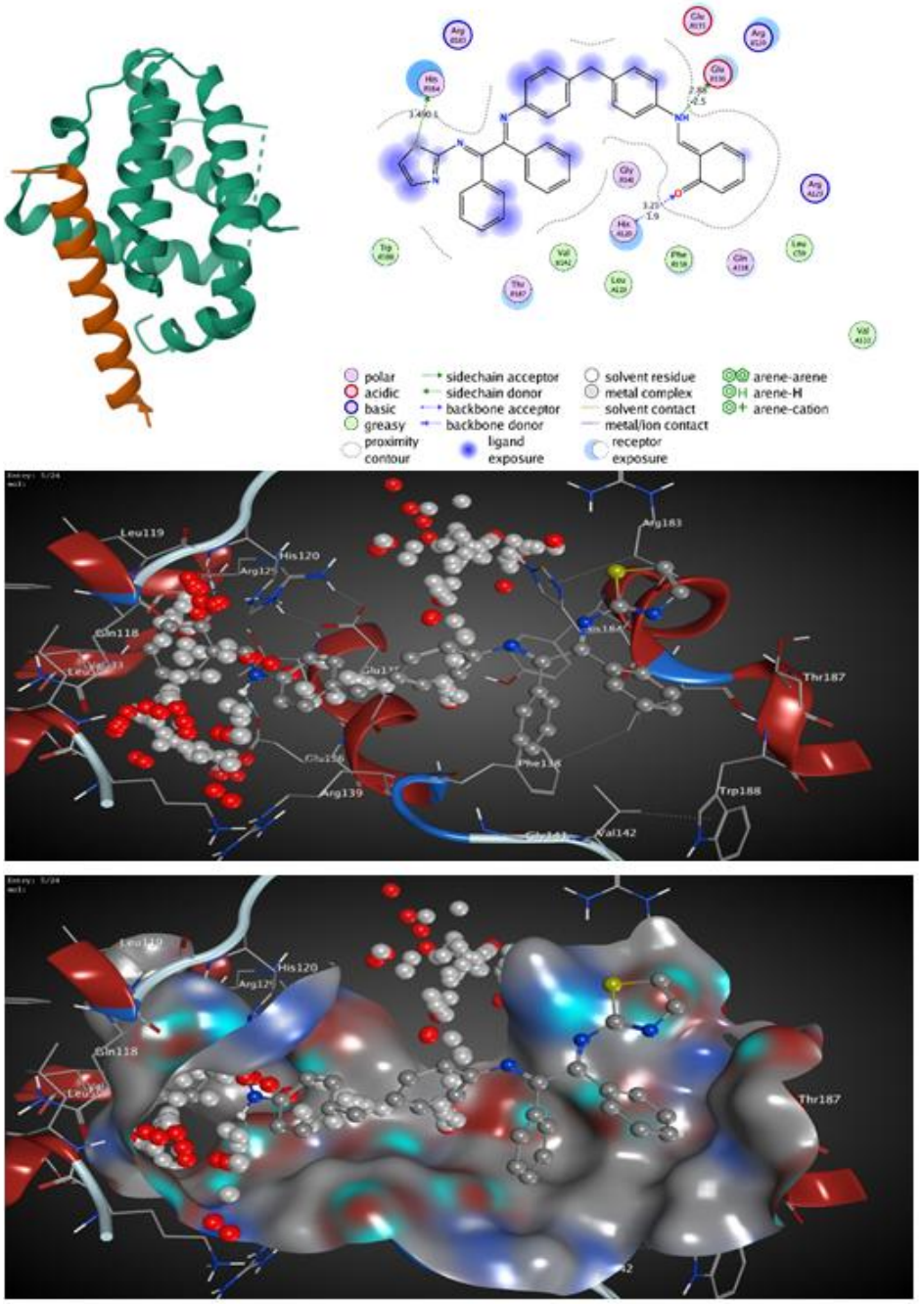

Fig. 11. Molecule Docking between IDB with protein 2XA0, utilizing 2D, 3D, and map views.

approximately 92.7% of amino acid residues were localized in energetically favored regions (Fig 11 and yield a suitable protein conformation for molecular docking.The free Ligand (IDB) showed a strong affinity to the protein active site which is confirmed by binding free energy value with kcal/molS,≤-7.7402 This suggests that this process can be spontaneous and stable due to favorable bonding of the energies. This increase of binding affinity was primarily due to the formation of extra hydrogen-bond interactions in pocket region. The analysis of the individual interactions around docked ligands indicates a strong hydrogen bond between nitrogen N9 from ligand and oxygen OE2 (oxygen atom in side chain) coming from amino acid residue GLU136, with an extremely short interaction distance measured as 2.88 Å which play an assistive role for stabilization of complex formation. In addition, binding was ensured by one more hydrogen bond with HIS120 at a distance of 3.21 Å (Fig. 11).With this methodology, ligands are embraced in relatively stable conformations within the active site with healthy flexibility (RMSD value of 1.8626 Å Fig. 12). However, 2023 showed the opposite binding method of Ag(II)-complex through mol2 docking. At a lower RMSD of 1.6313 Å, Protein cavity showed via geometrical stability better compact spatial orientation than the ligand and positive polar binding energy (−6.6690 kcal/mol) was shown less in complex compare to free form which is also functioned as energetic properties since they provide information for relationship between charge neutrality on induced surfaces at atomic level (Fig. 12).The enhanced rigidity of this complex was mainly linked to a transformation in the major-mode of interaction from classical hydrogen bonding↔ aromatic π–π stacking interactions. The coordination with silver center favors a more rigid molecular geometry, which enables aromatic rings of the complex interact functionally from 3.49 to 3.94 Åwith both imidazole rings of HIS184 and HIS120; in addition, The oxygen atom (O18) within the complex interacts forming an additional hydrogen bond contributing to stabilization powers towards ARG129 found into Active binding pocket as shown also on Table II. In general, a comparative analysis of the docking results indicates that coordination with silver has changed significantly in relation to the molecular recognition between ligand and receptor. Whereas the free ligand was dependent mostly on energetic contribution and flexibility of hydrogen-bond interactions, Ag(I)-complex succeeded in binding with enhanced geometric complementarity accompanied by steric stabilization within the cavity of protein. These results also suggest that the metal complex has a unique interaction signature and may have an increased capability to fit into the BCL-2 binding pocket, which further supports its potential as bioactive inhibitor with greater specificity in molecular targeting [27,28].

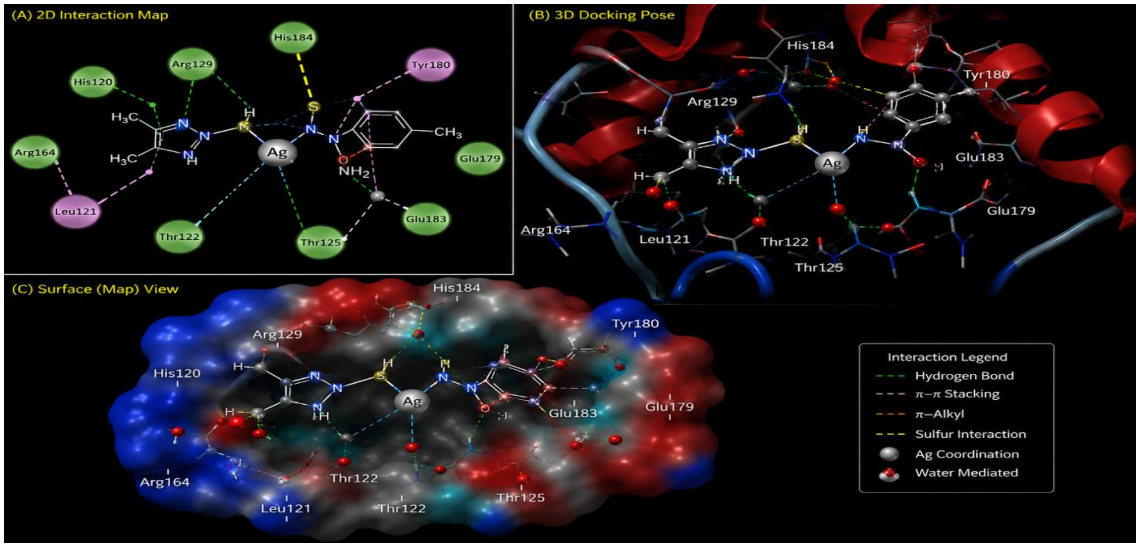

Fig. 12. 33D Molecular Docking Pose of Ag(I)-Complex within the active site of protein 2XA0.

CONCLUSION

The present study describes the synthesis and characterization of a new Schiff base ligand (SBOSA) with its silver complex using several spectroscopic methods, such as FT-IR, NMR, UV–Vis; physicochemical attributes: XRD; FESEM analysis and elemental analysis. The analytical results deduced were confirmed structures as proposed; coordination by azomethine nitrogen and oxygen donor atoms. In biological studies, free ligand and its [AgL] complex (silver focus) exerted antioxidant and cytotoxic actions in the A549 lung cancer cell line. However, the free ligand SBOSA possessed significantly higher cytotoxic potency and selectivity towards cancer cells than its Ag(II)-SBOSA complex. In addition, molecular docking studies revealed highly interacting residues at the BCL-2 protein active site further confirmatory experimental data and suggest anticancer potential through a stable binding nature of protein–ligand complex. The results suggest that the SBOSA structure and its silver complex could be new potential bioactive lead compounds to develop future novel active anticancer agents/ antioxidant products. In vivo studies and mechanistic investigations are warranted to understand their pharmacology and therapeutic potential.

CONFLICT OF INTEREST

The authors declare that there is no conflict of interests regarding the publication of this manuscript.

REFERENCES

1. Carta M. Cocaine inhibits 5-HT3 receptor function in neurons from transgenic mice overexpressing the receptor. Eur J Pharmacol. 2003;459(2-3):167-169.
2. Qin W, Long S, Panunzio M, Biondi S. Schiff Bases: A Short Survey on an Evergreen Chemistry Tool. Molecules. 2013;18(10):12264-12289.
3. Hameed G, Wadday F, Farhan M, Hussain S. Synthesis, Spectroscopic characterization and bactericidal valuation of some metal (II) complexes with new Tridentate Heterocyclic Azo Ligand Type (NNO) Donor. Egyptian Journal of Chemistry. 2020;0(0):0-0.
4. Hsu C-Y, Hameed GF, Ahmad I, Kumar A, Ganesan S, Shankhyan A, et al. Nanomagnetic nickel complex based on salicylamide and l -proline ligands as an efficient heterogeneous catalyst for synthesis of tetrazoles. Nanoscale Advances. 2025;7(9):2663-2676.
5. Kornev VI, Alabdullah GF, Kropacheva TN, Batueva EV. Heteropolynuclear cobalt(II) and nickel(II) ethylenediaminetetraacetates in aqueous solutions of aminoethanoic acid. Russian Journal of Inorganic Chemistry. 2016;61(5):660-665.
6. Ghosh P, Mukhopadhyay TK, Sarkar AR. Interaction of divalent metal ions with uracil III. Complexes of MnII, FeII, CoII, NiII and CuII with uracil acting as bidentate ligand. Transition Met Chem. 1984;9(2):46-48.
7. Xavier DA, Srividhya N. Synthesis and Study of Schiff base Ligands. IOSR Journal of Applied Chemistry. 2014;7(11):06-15.
8. Reedijk J. Bioinorganic Chemistry. Reference Module in Chemistry, Molecular Sciences and Chemical Engineering: Elsevier; 2013.
9. Chikhalia KH, Patel MJ, Vashi DB. Design, synthesis and evaluation of novel quinolinyl chalcones as antibacterial agents. ARKIVOC. 2008;2008(13):189-197.
10. McCleverty JA, Meyer TJ. Preface. Comprehensive Coordination Chemistry II: Elsevier; 2003. p. xv-xxiv.
11. Pervaiz M, Shahin M, Ejaz A, Quratulain R, Saeed Z, Ashraf A, et al. An overview of Aniline-Based Schiff base metal Complexes: Synthesis, characterization and biological activities - a review. Inorg Chem Commun. 2024;159:111851.
12. Venugopala KN, Jayashree BS. Microwave-induced synthesis of schiff bases of aminothiazolyl bromocoumarins as antibacterials. Indian J Pharm Sci. 2008;70(1):88.
13. Hasani N, Najim Abid Al-jibouri M. Synthesis, characterization, and DFT study of some transition metal complexes with Schiff base derived from 2-acetylthiophene and l-methionine. Res Chem Intermed. 2017;43(8):4585-4610.
14. Camellia FK, Ashrafuzzaman M, Islam MN, Banu LA, Zahan MK-E. Isoniazid Derived Schiff Base Metal Complexes: Synthesis, Characterization, Thermal Stability, Antibacterial and Antioxidant Activity Study. Asian Journal of Chemical Sciences. 2022:23-36.
15. Salian VV, Narayana B, Sarojini BK, Kumar MS, Nagananda GS, Byrappa K, et al. Spectroscopic, single crystal X-ray, Hirshfeld, in vitro and in silico biological evaluation of a new series of potent thiazole nucleus integrated with pyrazoline scaffolds. Spectrochimica Acta Part A: Molecular and Biomolecular Spectroscopy. 2017;174:254-271.
16. Rosnizam AN, Hamali MA, Muhammad Low AL, Anouar EH, Youssef HM, Bahron H, et al. Palladium(II) complexes bearing N,O-bidentate Schiff base ligands: Experimental, in-silico, antibacterial, and catalytic properties. J Mol Struct. 2022;1260:132821.
17. Yusuf TL, Oladipo SD, Zamisa S, Kumalo HM, Lawal IA, Lawal MM, et al. Design of New Schiff-Base Copper(II) Complexes: Synthesis, Crystal Structures, DFT Study, and Binding Potency toward Cytochrome P450 3A4. ACS Omega. 2021;6(21):13704-13718.
18. Gul Z, Din NU, Khan E, Ullah F, Nawaz Tahir M. Synthesis, molecular structure, anti-microbial, anti-oxidant and enzyme inhibition activities of 2-amino-6-methylbenzothiazole and its Cu(II) and Ag(I) complexes. J Mol Struct. 2020;1199:126956.
19. Gulcin İ, Alwasel SH. DPPH Radical Scavenging Assay. Processes. 2023;11(8):2248.
20. Liang N, Kitts D. Antioxidant Property of Coffee Components: Assessment of Methods that Define Mechanisms of Action. Molecules. 2014;19(11):19180-19208.
21. Nasaruddin NH, Ahmad SN, Sirat SS, Tan KW, Zakaria NA, Mohamad Nazam SS, et al. Synthesis, Structural Characterization, Hirshfeld Surface Analysis, and Antibacterial Study of Pd(II) and Ni(II) Schiff Base

Complexes Derived from Aliphatic Diamine. ACS Omega. 2022;7(47):42809-42818.
22. Kadhim SM, Mahdi SM. Preparation and Characterization of New (Halogenated Azo-Schiff) Ligands with Some of their Transition Metal Ions Complexes. Iraqi Journal of Science. 2022:3283-3299.
23. Gul Z, Salman M, Khan S, Shehzad A, Ullah H, Irshad M, et al. Single Organic Ligands Act as a Bifunctional Sensor for Subsequent Detection of Metal and Cyanide Ions, a Statistical Approach toward Coordination and Sensitivity. Crit Rev Anal Chem. 2023;54(7):2500-2516.
24. Ullah I, Ilyas M, Omer M, Alamzeb M, Adnan, Sohail M. Fluorinated triazoles as privileged potential candidates in drug development—focusing on their biological and pharmaceutical properties. Frontiers in Chemistry. 2022;10.
25. Yang M-Y, Zhao W, Sun Z-H, Tan C-X, Weng J-Q, Liu X-H. Synthesis and Biological Activity of Acylthiourea Derivatives Contain 1,2,3-thiadiazole and 1,3,4-thiadiazole. Letters in Drug Design and Discovery. 2015;12(4):314-318.
26. Herrera AM, García R, García G, Gastellóu E, Nieto F, Hirata GA, et al. Experimental determination of the pyrolysis temperatures of an organometallic complex to obtain AlxGa1-xN powders. J Alloys Compd. 2019;775:109-115.
27. Waheeb Azal S, Kyhoiesh Hussein AK. Ni(II) and Cu(II) Complexes With a Tridentate (O,N,O) Azo Dye Antipyrine-Based Ligand: Synthesis, Spectral Characterization, Cytotoxicity, and In Silico Approaches. Appl Organomet Chem. 2025;39(5).
28. Mahmood Taher A, Ali Kadhim Kyhoiesh H, Shakir Waheeb A, Al-Adilee KJ, Jasim LS. Synthesis, characterization, biological activity, and modelling protein docking of divalent, trivalent, and tetravalent metal ion complexes of new azo dye ligand (N,N,O) derived from benzimidazole. Results in Chemistry. 2024;12:101911.